Food and Chemical Toxicology 132 (2019) 110699

Contents lists available at ScienceDirect

Food and Chemical Toxicology

journal homepage: www.elsevier.com/locate/foodchemtox

Decursinol angelate ameliorates 12-O-tetradecanoyl phorbol-13-acetate (TPA) -induced NF-κB activation on mice ears by inhibiting exaggerated inflammatory cell infiltration, oxidative stress and pro-inflammatory cytokine production

Sukkum Ngullie Chang[a,1], Imran Khan[b,1], Debasish Kumar Dey[a], Kiu-Hyung Cho[c], Buyng Su Hwang[d], Ki Beom Bae[e], Sun Chul Kang[a,*], Jae Gyu Park[e,**]

[a] Department of Biotechnology, Daegu University, Gyeongsan, 38453, Republic of Korea
[b] Department of Biological Engineering, Biohybrid Systems Research Center (BSRC), Inha University, 100 Inha-ro, Nam-gu, Incheon, 22212, Republic of Korea
[c] Research group, Gyeongbuk Institute for Bio Industry(GIB), Andong, 36728, Republic of Korea
[d] Nakdonggang National Institute of Biological Resources, Sangju, 37242, Republic of Korea
[e] Advanced Bio Convergence Center, Pohang Technopark Foundation, Pohang, Gyeongbuk, 37668, Republic of Korea

ARTICLE INFO

Keywords:
Decursinol angelate
12-O-Tetradecanoylphorbol-13-acetate
Macrophage activation
Oxidative stress
NF-κB

ABSTRACT

Decursinol angelate (DA) is a pyranocoumarin purified from the roots of Angelica gigas. Here, we synthesized DA and determined its anti-inflammatory potential on TPA-induced mice ear inflammation. First, we evaluated the non-toxic behaviour of DA on HaCaT cells. Additionally, we observed the free radical scavenging potential of DA at 60 μM to be 50%. This finding was further supported by nitric oxide assay, malondialdehyde assay, H2DCFDA staining and western blotting analysis of antioxidant enzymes. DA also suppressed the activation and polarization of macrophage phagocytic activity on RAW 264.7 cells. We further evaluated the expression of ICAM-1, MCP-1, MIP-2 and MIP-1β on in-vivo model system. Consequently, DA significantly reduced the production of NF-κB and COX-2 induced proinflammatory cytokine levels on TPA induced ear edema. Inhibition of MAPK and transcriptional factor NF-κB was also validated by western blotting analysis of p-ERK, p-p38, IKKα, IKKγ, IκBα, NF-κB-p65. Immunohistochemistry and immunofluorescence staining of NFκB-p65, TNF-α and IL-1β were also performed to support the findings. Conclusively, these results suggest that topical administration of DA significantly inhibited the expression of pro-inflammatory cytokines by blocking the canonical NF-κB and MAPK pathway. Therefore, we suggest DA as a potent therapeutic compound against skin inflammation related diseases.

1. Introduction

Inflammation is a major driver of many diseases. It is often caused through the response of the immune system towards any stimuli it considers a threat, such as infectious micro-organisms, toxic compounds, irradiation or even the host's own damaged cell (Nathan and Ding, 2010). Different epidemiological studies have evidenced that inflammatory mediators are the major player having crucial role during the development of various diseases (P Libby et al., 2000; Korhonen et al., 2005; G S. Firestein, 2003) such as vascular diseases (G W. Sullivan et al., 2000), neurological diseases (D Degan et al., 2018), chronic inflammatory diseases (Straub and Schradin, 2016) and even in many different types of cancer (S I. Grivennikov et al., 2010). Whenever the immune system is challenged through some external stimuli, the first line of defence i.e innate immunity comes in role, such as macrophage activation. They are involved in the production many different types of pro-inflammatory cytokines. Among those produced by M1 macrophages are IL-1β, IL-4, IL-6, IL-12 and TNF-α. While, M2 macrophage produces IL-10 and also very low levels of IL-12 (Mosser and Edwards, 2008). Nitric oxide (NO) is also one of the main mediators of inflammation which stimulates the macrophage activation (J MacMicking et al., 1997). However, nuclear factor kappa B (NF-κB) is

* Corresponding author.
** Corresponding author. Advanced Bio Convergence Center, Pohang Technopark Foundation, Pohang, 37668, Republic of Korea.
E-mail address: sckang@daegu.ac.kr (S.C. Kang).
[1] Contributed equally to this work.

https://doi.org/10.1016/j.fct.2019.110699
Received 21 June 2019; Received in revised form 17 July 2019; Accepted 23 July 2019
Available online 24 July 2019

the primary signalling pathway involved in the process of initiating and amplifying inflammation (Li and Verma, 2002; Q Zhang et al., 2017). NF-kB is a paradigm of rapid response factor that comes out of the latency from the cytoplasm in the cell when there is an inflammatory insult or intrusion in a cell. The entire pathway is activated by an orderly response unit, such as B cell activation, cells of innate immune system are first activated by NF-kB at the site of inflammation, injury or infection (Y Ben Neriah, 2002). NF-kB is a nuclear transcription factor, it has the capability to modify the cell's biology by activating or repressing hundreds of target genes and it plays a central role in the onset of inflammation (Hayden and Ghosh, 2012). Thereby, NF-κB is directly involved in the regulation as well as the expression of various inflammatory genes including IL-1β, TNF-α, and COX-2, leading to an activated mitogen-activate protein kinases (MAPKs) pathway by TNF-α, which can activate all the three groups of MAP kinase extracellular signal-regulated kinase (ERK1/2), c-Jun N-terminal kinase (JNK) and p38 (Guadalupe and Davi, 2014).

Decursinol angelate belongs to the genus *Angelica L. of* the family of Umbellifera, isolated and extracted from the roots of *Angelica gigas Nakai* and other plants. The genus *Angelica L.* contains more than 60 species (Chen and Yang, 2004). The coumarin compound from the roots of *Angelica gigas* has been a subject of comprehensive research because of its potent therapeutic properties. Shehzad et al. has reported that decursin and Decursinol angelate (A Shehzad et al., 2018) have shown great potential in treating various chronic inflammatory diseases. Several studies have reported potential role the NF-κB inhibition by decursin and DA on different cancer cells and macrophage cells (J H. Kim et al., 2006; A Shehzad et al., 2016; S U. Islam et al., 2018; W J. Kim et al., 2010). The anti-inflammatory role of decursin derivatives has also been reported in mouse model of asthma (E J. Yang et al., 2009). Therefore, this study was carried out to comprehend the mechanism underlying the effects of DA on TPA induced ear inflammation mice model. To the best of our knowledge, we could not find any literature on *in-vivo* model of skin inflammation using DA. In this model, we had topically applied TPA as an inflammagen over a period of 4 days on mice ears, which induced epidermal hyperplasia and skin inflammation consisting of erythema, edema and infiltration of plasma and polymorphonuclear leukocyte (PMN) to the tissues that had undergone disrupted homeostasis. The symptoms of which are similar to persistent chronic skin inflammation (Tang and Wang, 2016). DA was able to inhibit the macrophages from polarizing and differentiating in RAW 264.7 cells. We observed that administration of DA to mice ears topically resulted in significant inhibition of TPA-induced ear erythema and edema. DA was also able to reduce the expression of different pro-inflammatory cytokines (TNF-α, IL-1β, and IL-6) and enzymes (COX-2, iNOS) and MCP-1, MIP-2, MIP-1β, MDA from the mice inflamed ears. In addition, we found that NF–κB p65 translocation to the nucleus was blocked, and there was also significant reduction of TPA-induced MAPK activation. Therefore, DA can be a reliable plant extracted compound that can be considered as a potential therapeutic drug for the treatment of skin inflammation related diseases.

2. Materials and methods

2.1. Chemicals

TPA (12-O-tetradecanoylphorbol-13-acetate), DMEM, 3-(4,5-dimethylthiazol-2-yl)-2,5-diphenyltetrazolium bromide (MTT), DAPI (4′,6-diamidino-2-phenylindole), dichlorodihydro -fluorescein diacetate (H_2DCFDA), dimethylsulfoxide (DMSO) were purchased from Sigma-Aldrich, St. Louis, USA. Fetal bovine serum was supplied by Gibco, USA. Primary antibodies β-actin, p-p38, p-ERK, COX2, n-NOS, i-NOS, e-NOS, TNF-α, NFκB p65 were purchased from bioworld technology, Inc. All other chemicals and reagents were of the highest analytical grade available. The details of primary and secondary antibodies used in the study were given in the Supplementary Tables 1A–B.

2.2. Synthesis of decursinol angelate

In order to synthesize DA, we prepared the crude extract from the roots of *Angelica gigas* (100 g) as previously described (J Lim et al., 2001). All the reactions were performed under inert atmosphere (argon or nitrogen) and glassware were oven-dried prior to use. Briefly, the homogenized root sample of the plant was dissolved in 70% of Ethanol (solvent) and allowed to boil for 8 h at 60 °C. After boiling, the mixture of solvent was filtered and extracted. The extraction procedure was performed for 3 times and later we concentrated the crude sample using rotary evaporator at 40 °C and recovered the extract using lyophilizer. Further, to purify decursinol from the crude extract, we dissolved the sample in MeOH/H_2O at a dilution of (1:1), and K_2CO_3 was added to the crude extract and kept at 100 °C for 24 h for reflux. The mixture was then cooled, and EtOAc was added in order to separate the organic and hydrophilic layers. The organic layer was further concentrated using $MgSO_4$ and the residue was purified by column chromatography. The total yield of decursinol was 56%, melting point: 177–179, R_f = 0.2 (Hexane:EtOAc = 1:1). ^{1}H NMR ($CDCl_3$, 400 MHz) δ 7.51 (d, 1H, J = 9.4 Hz, H_4), 7.11 (s, 1H, H_5), 6.70 (s, 1H, H_{10}), 6.15 (d, 1H, J = 9.6 Hz, H_3), 3.81 (t, 1H, J = 5.2 Hz, H_7), 3.04 (dd, 1H, ^2J = 16.8 Hz, ^3J = 4.8 Hz, H_{6A}), 2.77 (dd, 1H, ^2J = 16.8 Hz, ^3J = 5.6 Hz, H_{6B}), 1.90 (br. s, OH), 1.33 (s, 3H), 1.29 (s, 3H), ^{13}C NMR ($CDCl_3$, 100 MHz) δ 161.4, 156.5, 154.2, 143.2, 129, 116.5, 113.3, 112.9, 104.8, 78.2, 69.1, 30.7, 25.1, 22.1.

To further isolate and purify decursinol angelate from decursinol, we mixed 1 g of decursinol (4.06 mmol) with 992 mg of (*N,N*-dimethylamino) pyridine (DMAP, 8.12 mmol), and 481 mg of (*Z*)-2-methylbut- 2-enoyl chloride (4.06 mmol) in 30 ml of CH_2Cl_2, and kept in stirring condition for 24 h at 0 °C under nitrogen. Followed by the dilution of sample mixture with EtOAc (50 ml) and washed with saturated $NaHCO_3$ solution (30 mL), 0.1% HCl solution (30 mL), and water (30 mL) at the end. The organic layers were dried over $MgSO_4$, filtered and evaporated under reduced pressure. After removal of solvent, the resulted residue was purified by column chromatography (n-hexane: EtOAc = 1:1) with silica gel (230–400 mesh particle size, pore size 60 Å, Merck). The reactions were monitored by thin-layer chromatography (TLC) on commercial aluminum plates pre-coated with silica gel 60 (F-254, Merck). For further validation, the dried TLC plate was dipped in freshly prepared potassium permanganate solution (0.5% KMnO4 in 1 N NaOH) and immediately visualized under UV light at 254 nm. Purity of the compound was further analysed by NMR spectra, which were obtained using a Bruker-250 spectrometer 250 MHz or 400 MHz for ^{1}H NMR and 62.5 MHz or 100 MHz for ^{13}C NMR, reported as parts per million (ppm) from the internal standard tetramethylsilane (TMS). Chemicals and solvents were of commercial reagent grade and used without further purification. Elemental analyses were taken on Hewlett-Packard model 185B elemental analyzer. The yield of decursinol angelate was 82%, Melting point 79–80 °C (lit.[23] 78–80 °C), R_f = 0.7 (hexanes: EtOAc = 1:1). ^{1}H NMR ($CDCl_3$, 400 MHz) δ 7.57 (d, 1H, J = 9.2 Hz, H_4), 7.14 (s, 1H, H_5), 6.81–6.79 (m, 1H, $H_{3'}$), 6.79 (s, 1H, H_{10}), 6.19 (d, 1H, J = 9.4 Hz, H_3), 5.12 (t, 1H, J = 4.8 Hz, H_7), 3.28 (ddd, 1H, ^2J = 16.8 Hz, ^3J = 4.8 Hz, ^4J = 1.2 Hz, H_{6A}), 2.92 (dd, 1H, ^2J = 16.8 Hz, ^3J = 5.0 Hz, H_{6B}), 1.77–1.74 (m, 6H), 1.39 (s, 6H). ^{13}C NMR (acetone-d_6, 100 MHz) δ 167.2, 160.9, 157.3, 155.2, 144.3, 138.5, 130.2, 129.2, 117, 113.9, 113.8, 104.6, 79.2, 77.7, 71, 25.2, 23.5, 14.3, 12.1.

2.3. DPPH free radical scavenging assay

The free radical scavenging properties of the DA was determined using 1,1-Diphenyl-2-picrylhydrazyl (DPPH) assay (Dey et al., 2019). In this assay, ascorbic acid (10 μM) was considered as a positive control. In 96-well biochemical assay plate, different concentrations of DA (10, 30, 60 μM) and ascorbic acid were treated with 200 μl of the ethanolic DPPH solution, followed by incubation in dark for 30 min at room

temperature; the absorbance was then measured at 517 nm by using a spectrophotometer (UV-2120 Optizen, Mecasys, South Korea).The scavenging ability of the free radical was calculated as follows:

$$\text{Scavenging ability } \%= 1 - \frac{\text{At}}{\text{A0}} x100X$$

where At and A0 represent the readings of the sample and blank, respectively, at 517 nm.

2.4. Cell culture

Normal human keratinocyte cell (HaCaT) and murine macrophage cell line RAW 264.7 were cultured in DMEM supplemented with 10% fetal bovine serum and 1% penicillin-streptomycin on 37 °C incubator and facilitated with 5% CO_2.

2.5. MTT assay

The cytotoxicity of DA on HaCaT cells was evaluated by 3-(4,5-dimethylthiazol-2-yl)-2,5-diphenyl tetrazolium bromide (MTT) assay. Briefly, cells were cultured in 96 well plates at a density of 3×10^4 cells/ml and incubated at 37 °C humidified and 5% CO_2 incubator. After 48 h when the cells had reached 65–70% confluency the cells were treated with DA at varying concentrations. After 24 h of incubation, 10 μl of MTT (3-(4,5-demethylthiazol-2-3yl)-2,5-dephenyltetrazolium bromide, 5 mg/ml) reagent was added to each well along with 100 μl of DMEM and allowed to incubate for 3 h at room temperature. The culture medium containing MTT was discarded carefully and 50 μl of DMSO (dimethyl sulfoxide) was added to all wells and shaken in the dark for 30 min at room temperature for proper dissolution of the formed formazan products. The optical density for each well was measured at 570 nm wavelength using a microplate reader (TECAN 200 infinite PRO).

2.6. Role of DA on macrophage cells

To evaluate the effect of DA on macrophage cells, we treated murine macrophage RAW 264.7 cells with TPA (10 nM) (C. Wang et al., 2003) prior to DA treatment with different concentration (10, 30, 60 μM). Further we evaluated the effect of TPA and DA on the cell density using MTT assay and membrane fluidity using neutral red uptake assay as previously described (X Li et al., 2012; W Chen et al., 2010, Chauhan et al., 2014). Briefly, RAW 264.7 cells (3×10^4 cells/ml) were seeded into 96 well plates. After 48 h, cells were treated with TPA (10 nM). After 12 h of incubation TPA pre-treated cells were incubated with various concentrations of DA (10, 30, 60 μM) and incubated for next 24 h at 37 °C humidified and 5% CO_2 incubator. After the incubation period, the supernatants were discarded and 200 μl of 0.075% neutral red was added to all the wells and further incubated for 30 min at 37 °C. The neutral red solution was aspirated after 30 min and the wells were rinsed with 200 μl of PBS for 3 times with careful precision. The cells in the wells were lysed with 200 μl of 100 mM acetic acid: dehydrated alcohol = 1:1 (v/v) and incubated for 8 h at 4 °C for sufficient schizo analysis of the cells and for the release of phagotrophic neutral red. After 8 h, the optical density was measured at 490 nm wavelength using a microplate reader (TECAN 200 infinite PRO). The extent of phagocytosis and macrophage activation was expressed through the OD values.

2.7. TPA-induced skin inflammation and histology

Male 6–8 weeks old BALB/c mice were purchased from the Orient Bio, Inc. (Seoul, South Korea). The mice were housed in the animal breeding center of Pohang Technopark and were kept at room temperature of 20 ± 2 °C, relative humidity of 50 ± 5% and light intensity of 12 h using a constant temperature and humidity device. Prior to starting this study, all animal-related experiments were conducted after obtaining approval from the Pohang Technopark Laboratory Ethics Committee (approval number ABCC2018004).

The skin inflammation was induced on the left and right ear of each mouse (n = 5) by topical application of TPA as previously described (H Y. Song et al., 2008; Sun Hwa. Lee et al., 2012; E H. Ahn et al., 2010). TPA (10 μg) was used as an inflammagen which was dissolved in 20 μl of acetone and applied to the inner and outer surfaces of the mice ears every 24 h for 4 days. Following 1 h of TPA treatment, DA was applied topically on the ears of the mice. Next, after 1 h of DA treatment to the ears, its thickness was measured using a digital thickness gauge (Mitutoyo, Tokyo, Japan). On the final fourth day, we sacrificed the mice and the whole ear weight was measured and a 8-mm diameter punch was made in each mice to collect the tissue for the histological analysis.

2.8. Hematoxylin and eosin staining

Ear biopsies were fixed in 4% paraformaldehyde and stored at 4 °C for a day. Tissues were embedded in paraffin and sectioned at a thickness of 8 μm after de-paraffinization and hydration. The slides were washed with distilled water and stained with hematoxylin for 10 min. Excess amounts of stain were removed with 1% HCl–EtOH solution, followed by washing with ammonia water and distilled water. Background counterstaining was performed with eosin, followed by ethanol and xylene washes, cover slip were added to the slides and was analysed under a light microscope (both at 20x and 40x resolution).

2.9. Western blot analysis

In order to evaluate the protein expression before and after treatment of the mice tissue sample, we prepared the tissue lysate and loaded them on SDS- polyacrylamide gels. Proteins were resolved by electrophoresis and were transferred into a polyvinylidene difluoride membrane (PVDF). The blots were immersed in 5% non-fat milk prepared in PBS and incubated for 1 h, after which the membranes were probed with the antibody against the specific protein of interest for 2 h at 37 °C; followed by probing with an appropriate HRP-conjugated secondary antibody for 1 h at room temperature. All washes between and after incubations were done by wash buffer; after the final wash, blots were visualized using enhanced chemiluminescence Western blotting detection reagents (Amersham Biosciences Inc., Piscataway, NJ).

2.10. Quantitative analysis of cytokines

Ear tissues were homogenized with a protease inhibitor cocktail (Sigma–Aldrich, St. Louis, MO, USA) was incubated on ice for 15 min in the presence of 0.1% Triton X-100. The homogenate was further centrifuged at 15,000 × *g* for 10 min. After centrifugation, TNF-α, IFN-γ and IL-6, IL-1β, PGE_2, MCP-1, MIP-2 in the supernatants were measured by ELISA (R&D Systems Quantikine ELISA kits) and absorbance measured by TECAN spectrophotometry. The details of ELISA kits are mentioned in Supplementary Table 2.

2.11. Estimation of nitrite level in mice

The level of nitrite was estimated by using Griess Reagent (Sigma, USA). The ear tissue homogenized sample was mixed with Griess reagent in a ratio of 1:1, followed by incubation for 15 min at room temperature. After 1 h, absorbance was recorded at 540 nm using spectrophotometer (UV-2120 Optizen, Mecasys, South Korea). To determine the amount of nitrite, a standard curve was plotted using sodium nitrite as per the instructions of the Kit (G7921, Molecular Probes, life technologies, ThermoFisher, Austria). The standard curve was used for estimating the concentration of nitrite in each group of the samples.

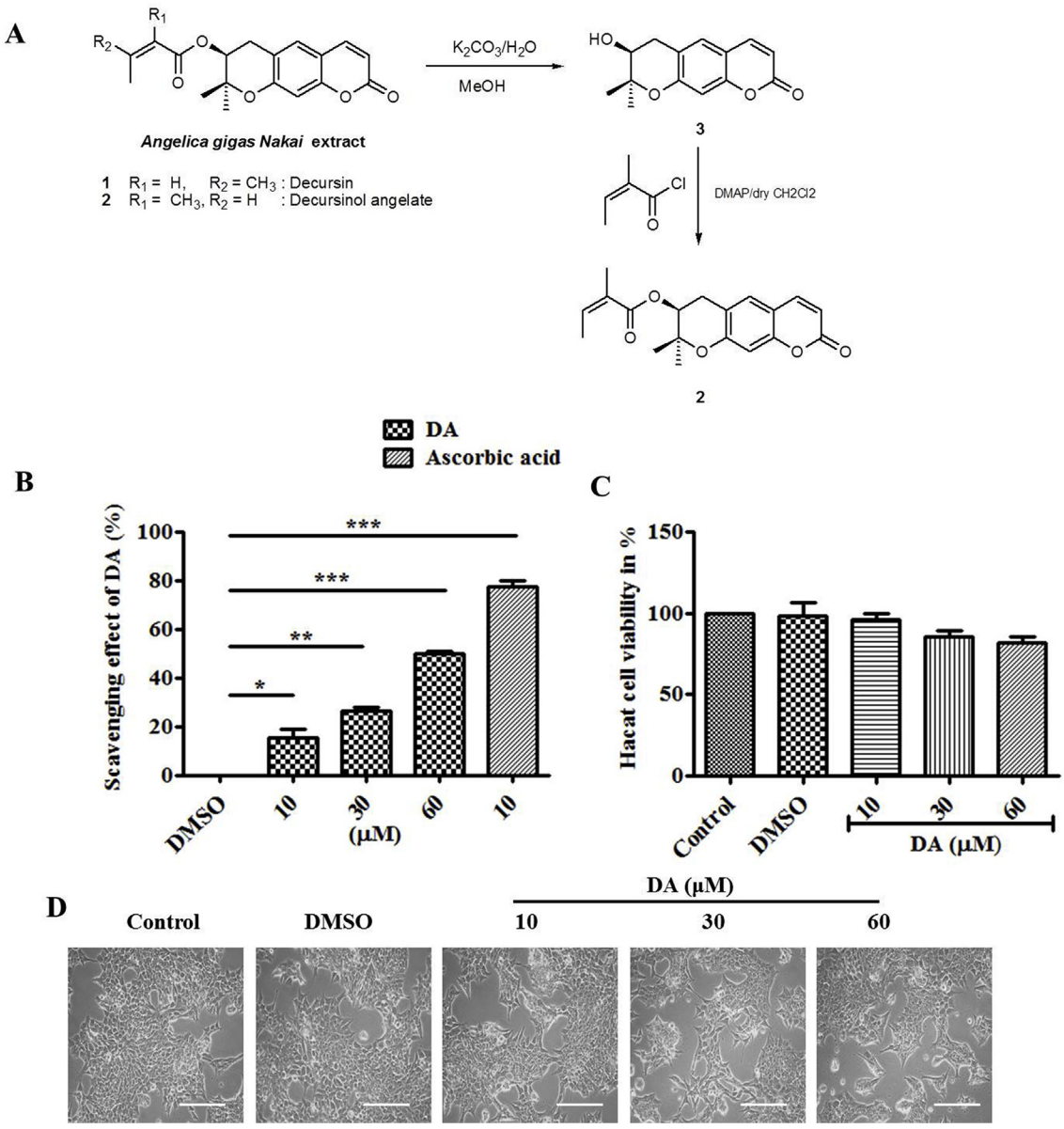

Fig. 1. DA exhibits non toxicity on HaCaT cells and Free radical scavenging potential (A) Preparation of Decursinol angelate from *Angelica gigas* extract (B) Free radical scavenging activity of DA on DPPH (C) MTT assay to evaluate the cytotoxicity of DA on normal human keratinocyte cells (HaCaT) (D) Structural morphology of HaCat cells after Treatment of DA at different concentration doses (10, 30, 60 μM) and DMSO (0.1%) control (no treatment). Scale bar (100 μm). The data are represented as the means ± S.D. of three independent experiments $*p < 0.05$, $**p < 0.01$, $***p < 0.001$ $***p < 0.00$. Statistical significance was analysed by prism ANOVA.

2.12. Estimation of lipid peroxidation in mice

The level of malondialdehyde (MDA) was measure using Malondialedehyde assay kit (Abcam). The homogenized ear tissue sample was mixed with 600 μl of thiobarbituric acid (TBA). The TBA-sample was incubated at 90 °C for 60 min in a hot water bath. After boiling, the samples were incubated at room temperature for 10–20 min on an ice bucket. 200 μl of TBA-sample reaction mixture was pipetted into a 96 well microplate. The absorbance was immediately measured at 532 nm wavelength.

The concentration of MDA was calculated as:

$$\text{MDA} = \left(\frac{\text{A}}{[\text{mg or ml}]}\right) \text{x } 4 \text{ x D} = \frac{\text{nmol}}{\text{mg}} \text{or} \frac{\text{nmol}}{\text{ml}}$$

Where, A = Amount of MDA in sample calculated from the standard curve (nmol). mg = Original tissue amount used (e.g. 10 mg). mL = Original plasma volume used (0.020 mL). 4 = Correction for using 200 μl of the 800 μL Reaction Mix. D = Sample dilution factor if sample is diluted to fit within the standard curve range (prior to reaction well set up).

2.13. Immunohistochemical staining

For immunohistochemical staining, de-paraffinized sections of ear biopsy blocks were used. The de-paraffinized slides were placed in xylene twice (each 5 min). The slides were transferred to 100% ethanol and kept thrice (3 min each). After 100% ethanol wash, slides were transferred to 95% ethanol for 3 min. The endogenous peroxidase activity was blocked by incubating slides for 10–15 min in H_2O_2 in PBS. The slides were than washed in PBS and kept under blocking buffer (Thermofisher scientific). The slides were incubated with primary antibodies (Bioworld Technology) for 3 h at room temperature. After

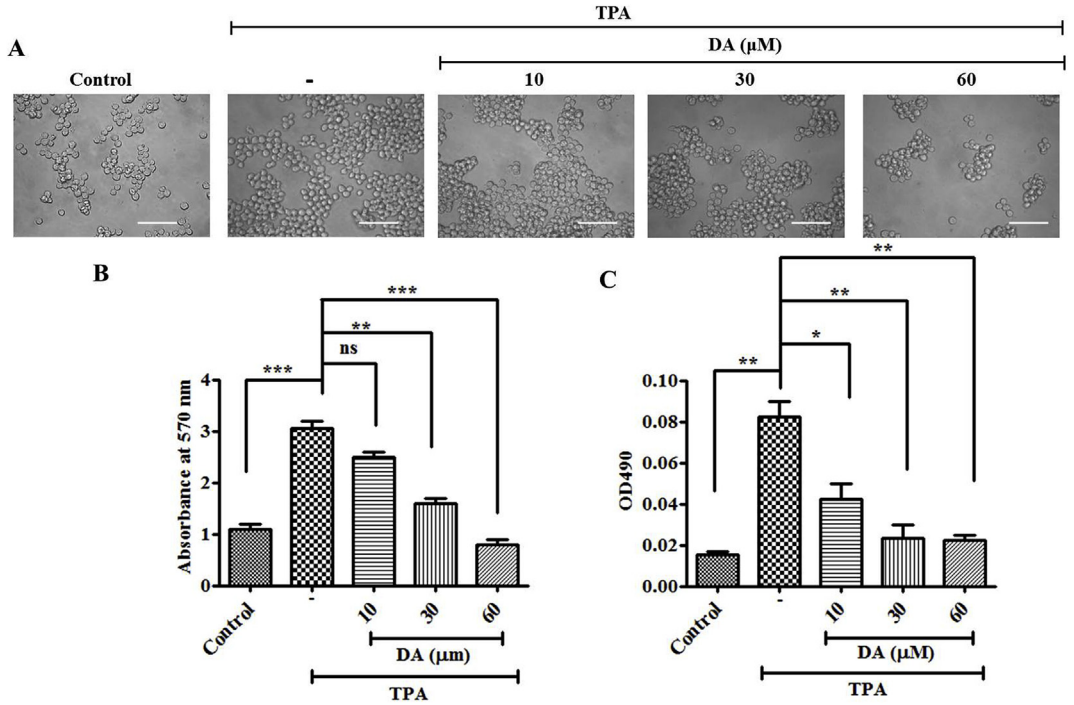

Fig. 2. DA reduces TPA induced macrophage activation on Mice ear biopsy and RAW 264.7 cells (A) Morphological analysis of Raw 264.7 cells 24 h after treatment with different doses of DA was compared with the TPA treatment (10 nM) (B) cell density was analysed by MTT assay at 72 h. (C) The effect of TPA on membrane fluidity of murine macrophage cell line was validated and its reduction was validated by dose dependent effect of DA using Neutral Red uptake assay. The data are represented as the means ± S.D. of three independent experiments *$p < 0.05$, **$p < 0.01$, ***$p < 0.001$, ***$p < 0.001$ and ns (non-significant). TPA vs control, DA 10 mg/kg and 25 mg/kg vs TPA. Statistical significance was analysed by prism ANOVA.

incubation, slides were washed with PBS (3 times) and incubated with secondary antibody for 30 min. DAB substrate solution was added to the slides and the slides were incubated for 15 min. The slides were rinsed in water and counterstained with hematoxylin for 30–60 s and the dehydration process was carried out after which the slides were fixed and observed under the microscope (Olympus BX51 Fluorescence Microscope).

2.14. Immunofluorescence staining

For immunofluorescence staining, the paraffin-embedded slides were permeabilized in 100%, 70%, 50% and 30% ice-cold methanol for 5 min each. After ethanol permeabilization, the slides were washed with Phosphate buffered saline with Tween-20 (PBST) twice for 10 min each followed by acetone permeabilization at −20 °C for 7 min. The slides were washed again with PBST for 10 min and incubated with the peroxidase blocking agent (methanol + DMSO + 15% H_2O_2) for 10 min. The slides were again washed with PBST and incubated in blocking agent PDT in 3% BSA 30 min. After blocking the slides were incubated in primary antibodies against NF-κB-p65 and TNF-α overnight at 4 °C. Next day the slides were washed 4 times with PDT and incubated in the dark for 2 h with FITC conjugated secondary antibody and counterstained with DAPI (1 μg/ml) for 30 min. The slides were washed with PBST and images were collected under the fluorescence microscope (Olympus BX51 Fluorescence Microscope).

2.15. Statistical analysis

The results for all the experiments in this study were expressed as a mean ± standard deviation (SD) of the experiments, and the statistical significance was calculated using ANOVA test from prism software; where *represents p-values < 0.05, **represents p-values < 0.01, and ***represents p-values < 0.001.

3. Results

3.1. Synthesis and antioxidant potential of DA

The schematic diagram represented in Fig. 1A shows the isolation process of DA from *Angelica gigas nakai extract.* The synthesized compound was further confirmed through HPLC and NMR analysis. NMR spectrum was very clean and the purity was over 99.5% with no bi-product. (Supplementary Fig. 1). In our study, DA was further evaluated for the antioxidant property represented in Fig. 1B. As observed, the percentage inhibition potential of DA (60 μM) was 50%, with a high statistical significant ($p < 0.001$) and thus, validates the hypothesis that DA could be beneficial to reduce the inflammation in the host body. The observed result was similar to the positive control taken in the assay. Ascorbic acid (10 μM) significantly ($p < 0.001$) scavenged the DPPH free radical from the micro environment. Therefore, the result demonstrated the antioxidant potential of DA.

3.2. Cytotoxic assessment of DA on normal human keratinocytes

To illustrate the potential of DA on the treatment of chronic skin inflammation, first, we ensured its toxicity for further applications. Therefore, we treated HaCaT cells with different doses of DA (10, 30, 60 μM), where DMSO (0.1%) was taken under consideration to normalize the effect of the solvent. The results from MTT assay for cell viability was observed to be normal at DMSO 0.1% (98.02%) compared to DA 10, 30 and 60 μM (95.85, 85.71, 84.87% respectively) having no significant difference ($p < 0.1163$). Morphological analysis (Fig. 1D) also revealed the non-cytotoxic behaviour of DA on the normal human keratinocytes. In addition, it does not show any significant changes in cell viability and density (Fig. 1C). The results confirmed and satisfied the safety concern for its further application against TPA induced inflammation *in-vitro* and *in-vivo* model.

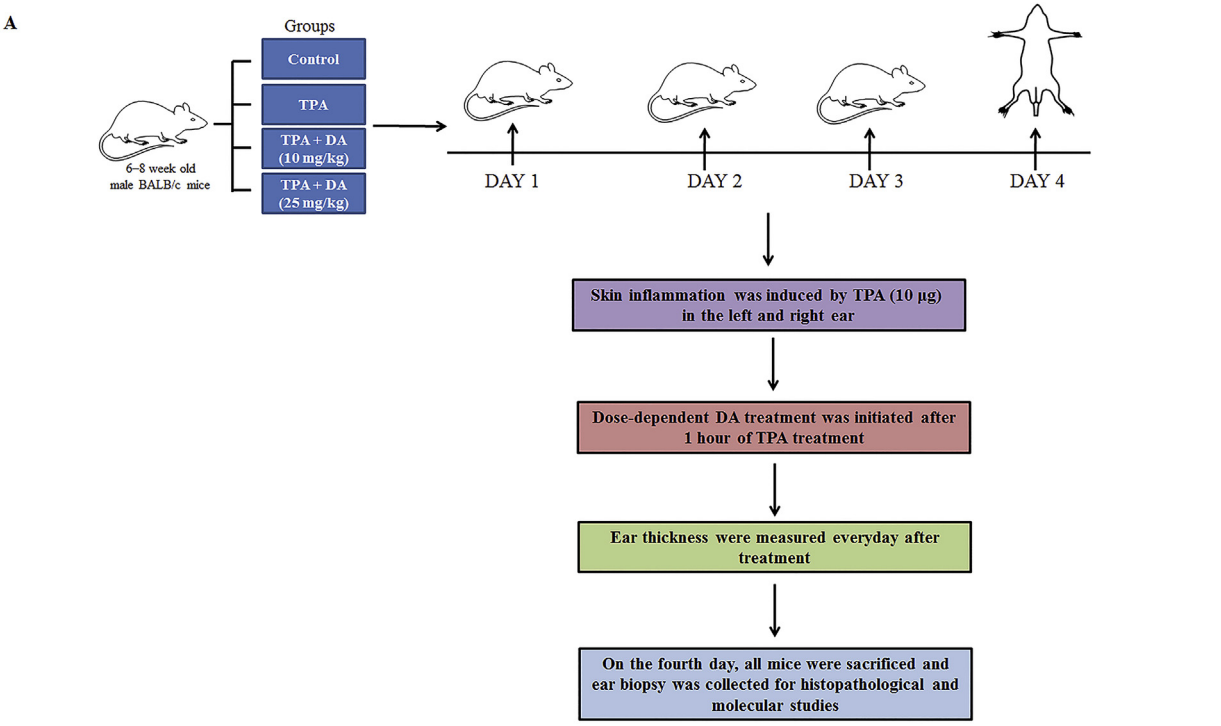

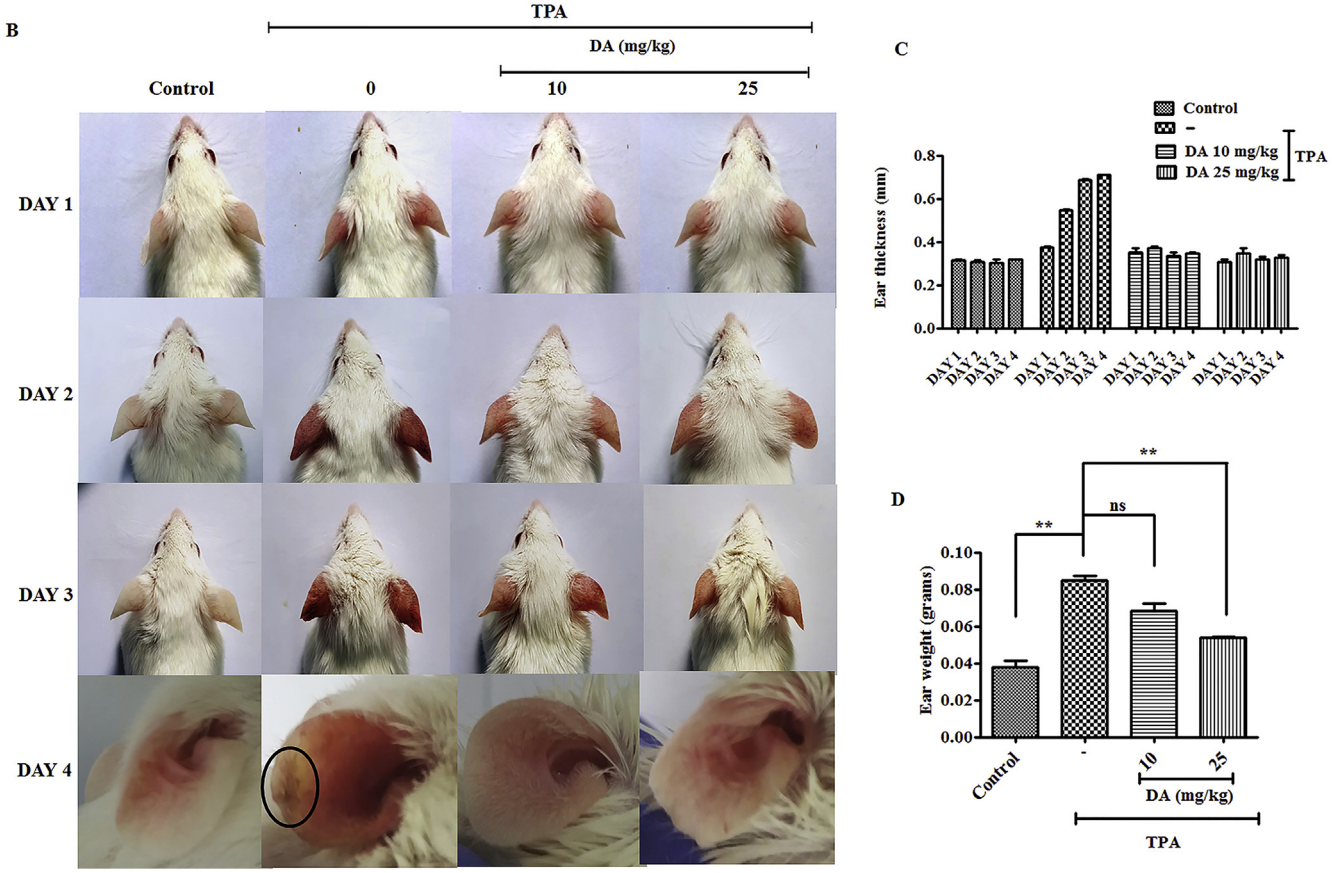

Fig. 3. DA Inhibits TPA induced epidermal hyperplasia and ear edema (A) Schematic representation of the experimental procedure. (B) Images of mice ear (n = 5) collected every day after TPA and DA treatment over a period of 4 days. (C) Inhibition of TPA induced epidermal hyperplasia and ear edema was analysed by measuring the following parameters. Ear thickness was measure every day after topical treatment of TPA and DA for 4 days (D) Ear weight of different mice group after sacrifice.

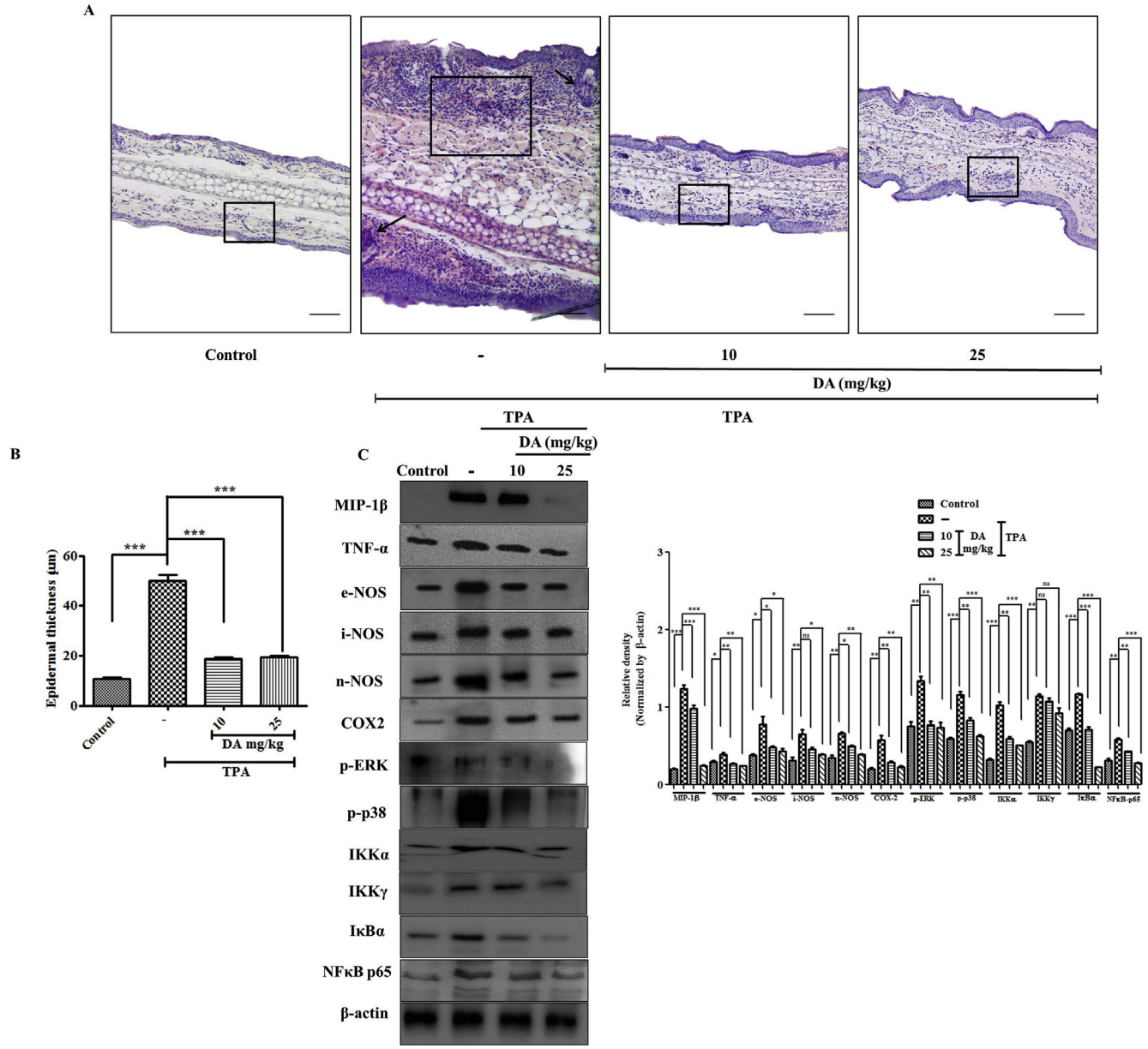

Fig. 4. DA ameliorates TPA induced epidermal hyperplasia and inhibits MAPK and NFκB pathway (A) H&E staining images of ear biopsy tissue. **Black arrow:** The regions in the black arrow indicates epidermal hyperplasia and re-epithelialization with newly formed, thick epidermis that was complete as observed on TPA alone group. **Square:** The regions under the square indicate massive aggregation of granulation tissue granulation tissue. It also occurs in all wounds during the healing process and it also occurs in chronic inflammation. It comprises of fibroblasts surrounded by abundant ECM, newly formed blood vessels, scattered macrophages, and some other inflammatory cells. (B) Measurement of epidermal thickness of different groups in μm. Scale bar (100 μm). (C) DA significantly reduced the inflammatory response challenged by TPA (10 μg/ear), which was validated through western blotting analysis. We observed a significant downregulation of MIP-1β ($p < 0.0001$), TNF-α ($p < 0.0049$), e-NOS ($p < 0.0178$), i-NOS ($p < 0.0114$), n-NOS ($p < 0.0012$), COX-2 ($p < 0.0028$), p-ERK ($p < 0.0041$), p-p38 ($p < 0.0004$), IKKα ($p < 0.0002$), IKKγ ($p < 0.0019$), IκBα ($p < 0.0001$), NFκB p65 ($p < 0.0007$) at DA 10 and 25 mg/kg treatment groups compared with TPA group. Densitometry analysis of the respective proteins was evaluated by Image J software, and results were normalized by β-actin. The data are represented as mean ± S.D. of three independent experiments $*p < 0.05$, $**p < 0.01$, $***p < 0.001$ and ns (non-significant). TPA vs control, DA 10 mg/kg and 25 mg/kg vs TPA.

3.3. Effect of DA on TPA-induced macrophage activation

To study the potential of DA against TPA induced macrophage activation, we performed MTT and neutral red uptake assay on RAW-246.7 cells. For MTT assay, the cells were pre-treated with TPA at 10 nM and then treated with DA at various concentrations (10, 30, 60 μM). To evaluate the morphological changes, we collected cell images after 24 h of treatment (Fig. 2A). The results of MTT assay shows a significant ($p < 0.0001$) activation of macrophage as observed on TPA treated group which was subsided after DA (60 μM) treatment (Fig. 2B). As one of the important factors in the uptake of particles by phagocytic cells is the membrane fluidity, so we also analysed the specific function of murine macrophages by neutral red uptake assay. The cells were treated with TPA (10 nM) and DA at varying concentrations (10, 30, 60 μM). After the addition of neutral red solution DA at 60 μM showed the significant ($p < 0.01$) activity in reducing the TPA induced macrophage activation giving an optical density of 0.017 in comparison with TPA (0.082, $p < 0.001$) treatment (Fig. 2C). The result was also further evaluated on mice ear tissues. Immunofluorescence staining of intercellular adhesion molecule (ICAM-1),

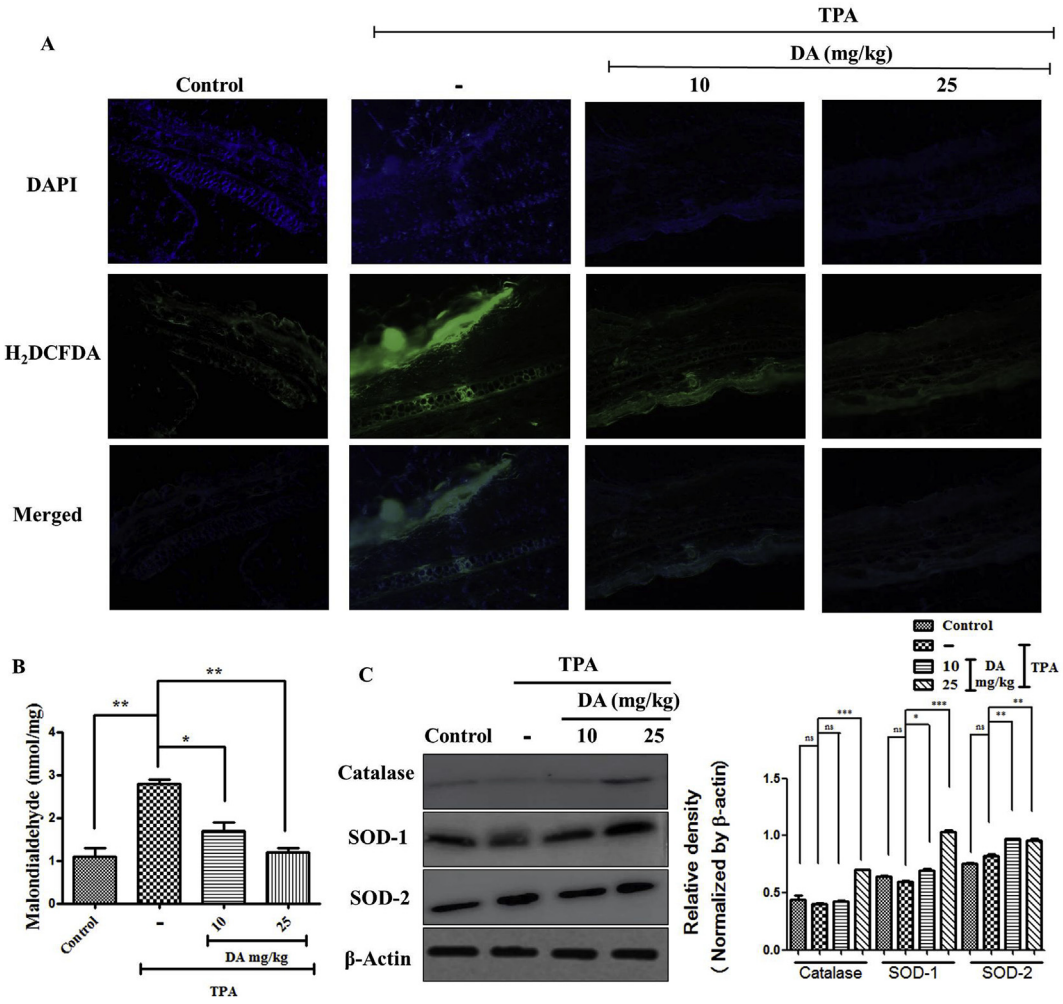

Fig. 5. DA inhibits ROS production and promotes antioxidant activity (A) Immunofluorescent detection of DCFH-DA on mice ear biopsy section. DCFH-DA is stained green and nucleus is stained blue with DAPI. Measurement of ROS by H_2DCFDA showed reduction of free radicals on DA (10–25 mg/kg) group as compared with TPA group. TPA alone group is shown to have more intense green fluorescence stain indicating more production of ROS, while the intensity of green fluorescence dye decreased on DA groups. Magnification = 20x. (B) Ear tissue samples were evaluated for Malondialdehyde production. (C) Western blotting analysis of antioxidant enzyme markers, Catalase ($p < 0.0012$), SOD-1 ($p < 0.0001$), SOD-2 ($p < 0.0006$). Densitometry analysis of the respective proteins was evaluated by Image J software, and results were normalized by β-actin. The data are represented as the means ± S.D. of two independent experiments $^{*}p < 0.05$, $^{**}p < 0.01$, $^{***}p < 0.001$ and ns (non-significant). TPA vs control, DA 10 mg/kg and 25 mg/kg vs TPA. (For interpretation of the references to colour in this figure legend, the reader is referred to the Web version of this article.)

which is highly expressed during macrophages activation (S F. Bernatchez et al., 1997) revealed that TPA treatment group had exaggerated overexpression of macrophages and infiltratory cells as compared with control and DA treatment groups (Fig. 6A), analysed through the uptake of more green fluorescence stain on TPA group. We also evaluated the levels of monocyte chemoattractant protein-1 (MCP-1) and macrophage inflammatory protein 2 (MIP-2) from mice ear tissue homogenates. It was found that TPA treatment group for both MCP-1 and MIP-2 had a higher expression concentration (404 pg/ml and 488.5 pg/ml) which were significantly lowered upon DA treatment for both DA 10 and 25 mg/kg (210, 171.5 pg/ml, $p < 0.0001$) and (162.65, 130.5 pg/ml, $p < 0.0001$). Western blotting (Fig. 4C) analysis for macrophage inflammatory protein1β (MIP-1β) also reduced in a dose dependent manner compared to TPA groups ($p < 0.0001$) indicating the role of DA in subduing Inflammatory cell infiltration triggered by TPA treatment.

3.4. Anti-inflammatory potential of DA on TPA-induced ear inflammation in mice ears

TPA has shown the potential to activate the macrophages in order to induce the inflammation (P L. Stanley et al., 1991; H Y. Ha et al., 2006). Therefore, we designed the *in-vivo* experiment to induced mice ear edema using TPA as a model for acute and chronic inflammation (Fig. 3A). Topical application of TPA (10 μg/ear) on BALB/c mice ear over a period of 4 days was shown to stimulate a skin inflammatory response consisting of erythema and edema (Fig. 3B). TPA treated group aggravated the swelling of ears, increased ear thickness and ear weight ($p < 0.01$) (Fig. 3 C, D). Topical application of DA, (10 and 25 mg/kg) after 1 h of TPA application once a day for 4 days ameliorated TPA induced ear edema and decreased the number of inflammatory cells in a dose dependent manner. The result was also further analysed through H&E staining (Fig. 4A), where TPA treated group showed increased re-epithelialization, epidermal hyperplasia, accumulation of granulation tissue, newly formed blood vessels and infiltration of inflammatory cells. There was also increased number of inflammatory cells infiltration at the TPA treatment regions of the ear and an increase in epidermal thickness (Fig. 4B). We observed a significant ($p < 0.001$) reduction of epidermal hyperplasia, inflammatory cells and epidermal thickness in the DA (10 and 25 mg/kg) treated groups indicating an effective anti-inflammatory potential of DA on *in-vivo* model system.

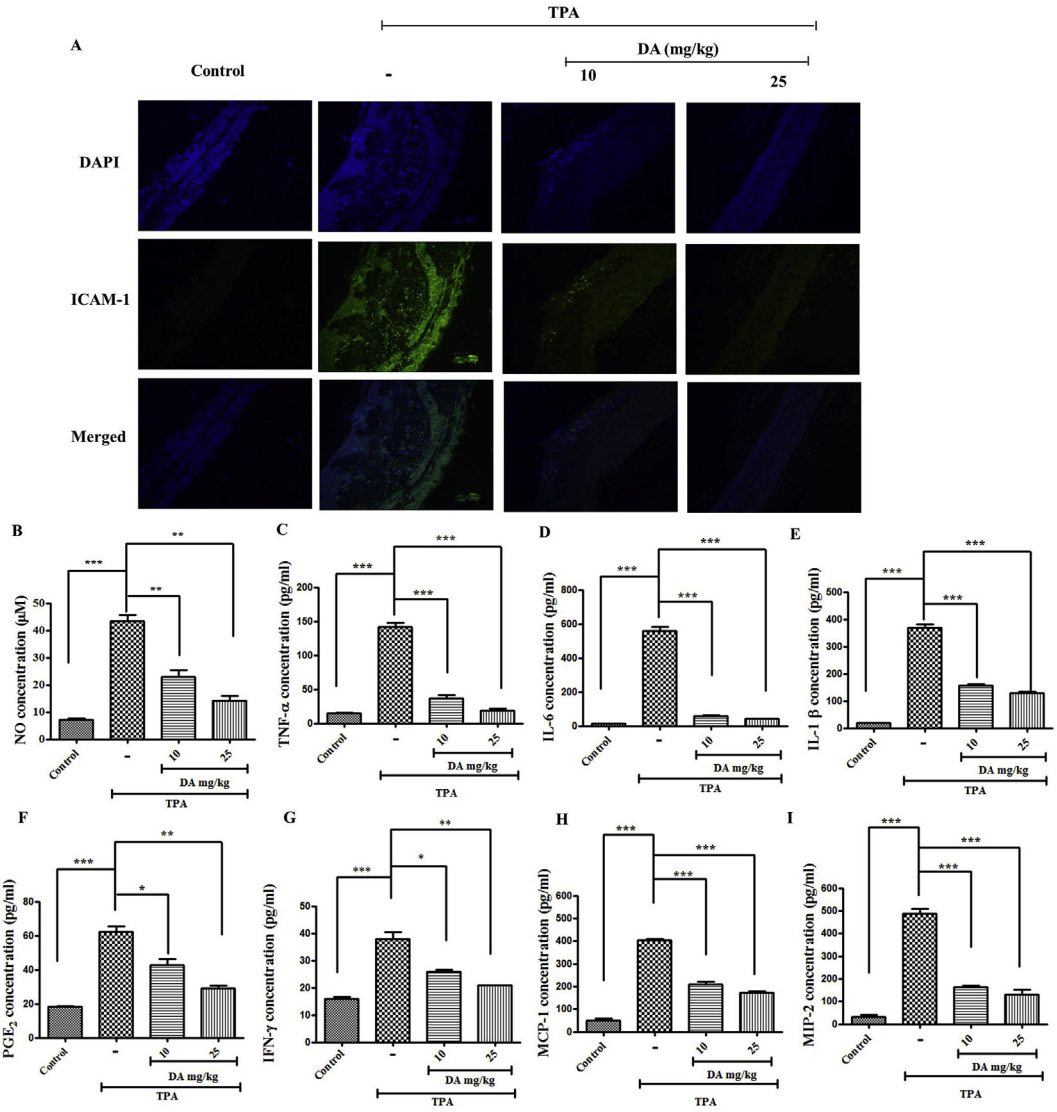

Fig. 6. DA suppresses TPA induced macrophage activation and inhibits production of different pro-inflammatory cytokines (A) Macrophage activation was analysed through ICAM-1 overexpression on mice ear biopsies. Immunofluorescent detection of ICAM-1 for macrophage polarization and activation. ICAM-1 is stained in green and nucleus is stained blue with DAPI. The experiment was performed to validate the activation of macrophage leading to highly expressed ICAM-1 on TPA treatment group which was analysed by the uptake of more green fluorescence stain on the ear biopsy tissue sections as compared with control (no treatment) and DA (10–25 mg/kg) group (n = 5 per group) Magnification = 20x. (B–I) Measurement of inflammatory cytokines from the ear biopsy tissues. Inhibitory effect of DA on TPA-induced inflammatory cytokines from the ear biopsy tissues in mice ears. Mice ears (n = 5) were treated with TPA (10 μg/ear) once a day for 4 days. DA (10 and 25 mg/kg) was topically applied to mice ears 1 h after TPA treatment. Mice ear extracts were prepared and analysed for pro-inflammatory cytokine expression. Supernatant fractions of homogenates from ear biopsies were examined for cytokine production using ELISA and NO assay, IL-6, TNF-α IL-1β, PGE_2, IFN-γ, MCP-1, MIP-2. The *p* values for TPA was compared with control and *p* value for sample DA 10 mg/kg and 25 mg/kg was compared with TPA. The data are represented as the means ± S.D. of three independent experiments $*p < 0.05$, $**p < 0.01$, $***p < 0.001$, $***p < 0.001$ and ns (non-significant). TPA vs control, DA 10 mg/kg and 25 mg/kg vs TPA. Statistical significance was analysed by prism ANOVA. (For interpretation of the references to colour in this figure legend, the reader is referred to the Web version of this article.)

3.5. Effects of DA on NF-κB and MAP kinase pathway on TPA-induced inflammation in mice ears

In order to trigger a pro-inflammatory cytokine response by immune cells, NF-κB and MAPK are the fundamental pathways that are needed to be activated (P Zhang et al., 2005; T Lawrence, 2009). Therefore, we topically applied TPA on the inner and outer regions of the mice ears for 4 days. After 1 h of TPA treatment, DA at a dose of 10 and 25 mg/kg was administered topically on the TPA treated region of mice ears. From the ear tissue homogenates, we performed a western blotting analysis of MAP kinase pathway markers such as p-ERK ($p < 0.0041$) and p-p38 ($p < 0.0004$) protein kinase. The phosphorylated ERK and p38 marker was markedly downregulated in a dose dependent manner on DA treatment groups, in comparison to TPA treatment only mice group (Fig. 4C). TPA also induced the activation of NF-κB, which is a well-known redox-sensitive transcription factor regulating the expression of many pro-inflammatory genes (T Liu et al., 2017; Bhatt and Ghosh, 2014). NF-κB p65 subunit expression was also downregulated in a dose-dependent manner in DA treatment groups observed through western blotting of IKKα ($p < 0.0002$), IKKγ ($p < 0.0019$), IκBα ($p < 0.0001$) and NFκB-p65 ($p < 0.0007$) (Fig. 4C). Further, we also assessed the transcriptional targets of NF-κB in the tissue sample by analysing their expression and comparing with the expression of control, TPA and DA treatment groups. Accordingly, we observed that the expressions of TNF-α ($p < 0.0049$), e-NOS ($p < 0.0178$), i-NOS ($p < 0.0114$), n-NOS ($p < 0.0012$), and COX2 ($p < 0.0028$) (Fig. 4C)

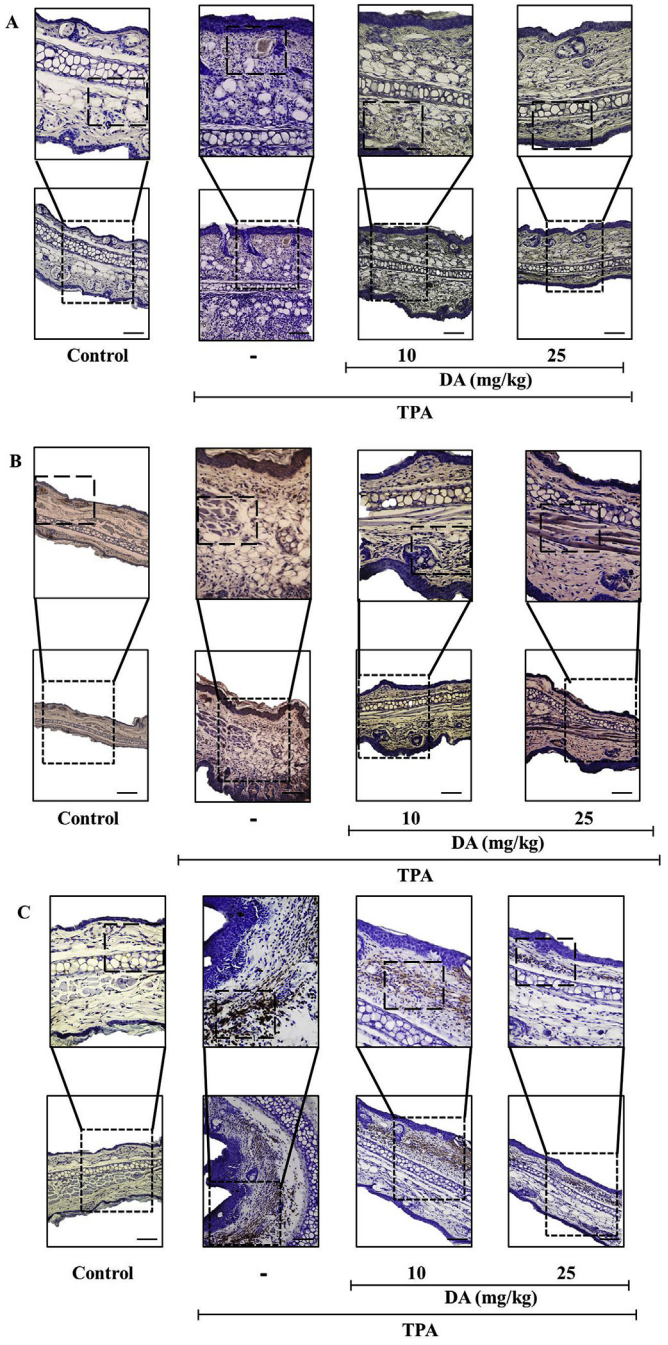

Fig. 7. Immunohistochemical staining of TPA treated ear biopsies after formalin fixation and paraffin-embedded sections (A) NF-κB p65 (B) TNF-α (C) IL-1β. TPA group had more concentration of NF-κB p65 as compared to DA (10–25 mg/kg) as determined through browning reaction observed in the stained tissue sections. Scale bar (100 μm). Magnification = 20x.

were significantly higher in the TPA treated group when compared to the control group. We also observed a significant dose dependent decrease in their protein levels after treatment with DA.

3.6. Effect of DA on the generation of reactive oxygen species

ROS is known to react directly with the double bonds of polyunsaturated fatty acids (PUFAs), leading to the production of lipid hydroxides which thereby contribute to the disruption of necessary biomolecules required for biological mechanisms (G Barrera, 2012). As per the Western blot analysis, we observed DA can significantly reduce the expression of NOS proteins, so we further evaluated the potential of DA to inhibit oxidative stress induced by TPA which generates more reactive oxygen species (A Q.Khan et al., 2013). The mice ear tissue homogenates were analysed for the production malondialdehyde (MDA), which is a major marker of oxidative stress (Draper and Hadley, 1990). We observed that DA groups 10 and 25 mg/kg (1.7 and 1.2 nmol/mg) was able to significantly reduce the production of MDA as compared with TPA group (2.8 nmol/mg) with a significant difference of ($p < 0.0050$) (Fig. 5B). The ear biopsy were also stained and analysed for the uptake of green fluorescent dye H_2DCFDA (A Sengupta et al., 2010). As illustrated in Fig. 5A, the intensity of green fluorescence markedly decreased in a dose-dependent manner in DA treated groups (10 and 25 mg/kg). Whereas, TPA treatment only group had an intense green fluorescence stain indicating a higher production of ROS. The results revealed a reduced level of reactive oxygen species generation after topical application of DA. We further performed NO assay, as depicted in Fig. 6B, TPA treated group showed significantly higher production of NO (43.05 μM) as compared to control group (7.13 μM). Topical application of DA (10–25 mg/kg) significantly reduced NO production on TPA challenged groups (22.93 μM and 14.21 μM) and a significant difference of ($p < 0.0006$) respectively. Concurrently, western blotting analysis of antioxidant enzymes (Fig. 6C), catalase ($p < 0.0012$), superoxide dismutase (SOD-1) ($p < 0.0001$) and manganese superoxide dismutase (SOD-2) ($p < 0.0006$) were also increased significantly on DA treatment groups. Collectively, the result of the experiment also supports the finding of Fig. 1B.

3.7. Effect of DA on the production of pro-inflammatory cytokines in TPA induced ear inflammation

In order to further validate the results of western blotting analysis, we performed ELISA and immunohistochemistry and immunofluorescence staining. The results of ELISA estimation are presented in Fig. 6 (C, D, E, F, G). TPA treatment aggravated the mice ears resulting in the over expression of pro-inflammatory cytokines, whereas, 10 and 25 mg/kg treatment of DA significantly reduced their production rate as observed. The level of TNF-α, IL-6, IL-1β, PGE_2, and IFN-γ was recorded lesser in the control group (18.38, 12.82, 369.56, 62.26 and 15.79 pg/ml) respectively. However, their level was found to be elevated in TPA induced inflammatory group (141.63 pg/ml, $p < 0.001$; 558.01 pg/ml, $p < 0.001$; 369.56 pg/ml, $p < 0.001$; 62.26 pg/ml, $p < 0.001$; and 37.93 pg/ml; $p < 0.001$) respectively. But after treatment with DA of 10 mg/kg and 25 mg/kg their level of significantly reduced (36.19 pg/ml, $p < 0.001$; 57.67 pg/ml, $p < 0.001$; 157.57 pg/ml, $p < 0.001$; 42.69 pg/ml, $p < 0.05$; and 25.8 pg/ml, $p < 0.05$) and (18.24 pg/ml, $p < 0.001$; 43.16 pg/ml, $p < 0.001$; 129.66 pg/ml, $p < 0.001$; and 29.15 pg/ml, $p < 0.01$; and 20.80 pg/ml, $p < 0.01$) respectively. Altogether, Topical application of DA (25 mg/kg) was found to be potent enough to inhibit the level of PGE_2, e-NOS, i-NOS, n-NOS and COX-2 in TPA-induced ear inflammation model system.

The results were also validated by immunohistochemistry analysis. As observed, the mice ear biopsy had revealed lesser accumulation of NF-κB-p65, TNF-α, and IL-1β on DA (10 and 25 mg/kg) in comparison with the TPA treated group, which had higher expression of these pro-inflammatory cytokines determined through brown reaction products (Fig. 7A and B, C).

In particular, to determine the impact of DA on NF-κB-p65, TNF-α expression, immunofluorescent staining was also performed. As shown in Fig. 8, the fluorescent intensity of both NF-κB-p65 (Fig. 8A) and TNF-α (Fig. 8B) were highly upregulated in TPA induced inflammatory model when compared to its respective control sample. Conversely, topical treatment of DA reduced the fluorescent intensity of NF-κB-p65 and TNF-α, providing the evidence of its inhibition capacity against the TPA induced ear inflammation. Taken together, this result indicates that DA could be a good therapeutic compound for different kinds of inflammatory diseases.

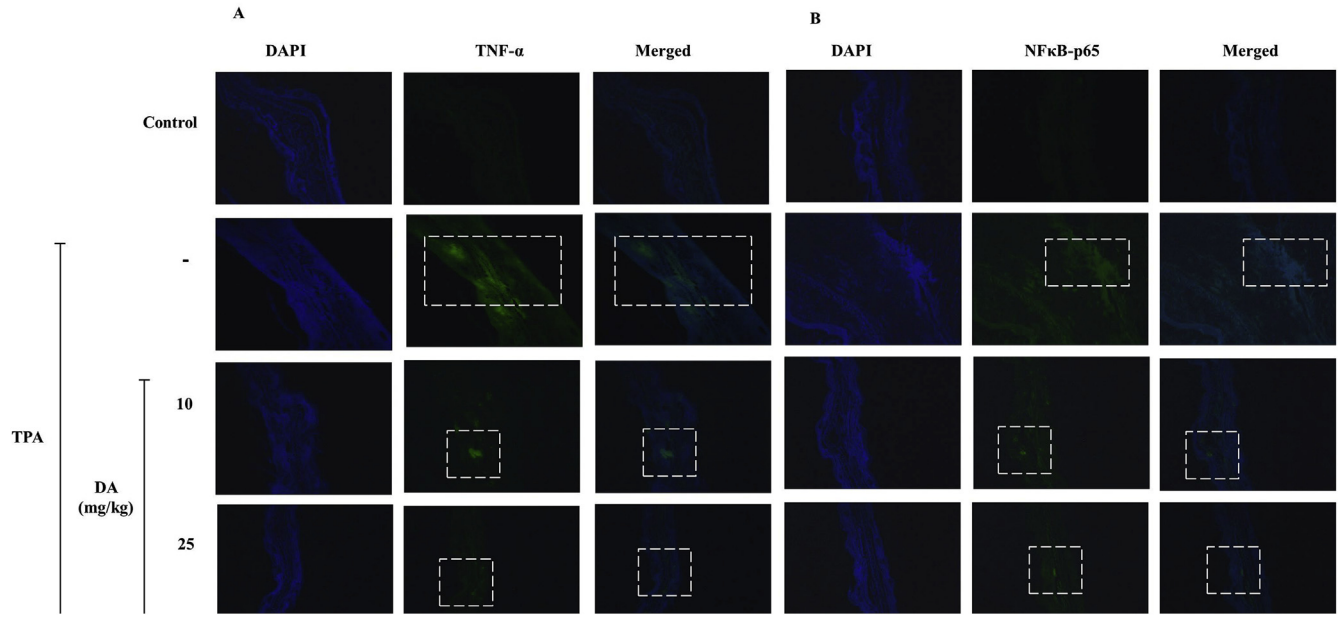

Fig. 8. Immunofluorescence staining of TPA treated ear biopsies after formalin fixation and paraffin-embedded sections (A) Immunofluorescent detection of TNF-α. TNF-α is stained in green and nucleus is stained blue with DAPI. (B) Immunofluorescent detection of NF-κB p65. NF-κB p65 is stained in green and nucleus is stained blue with DAPI. The experiment was conducted in order to validate the inhibition of TNF-α and NF-κB-p65 expression by DA (10–25 mg/kg) as compared with TPA only group which was analysed by the uptake of more green fluorescence stain on the ear biopsy tissue sections. (n = 5 per group) Magnification = 20x. (For interpretation of the references to colour in this figure legend, the reader is referred to the Web version of this article.)

4. Discussion

Angelica gigas is a medicinal plant of Korean origin, having high amounts of DA as compared to other Dangui of Chinese and Japanese origin. We synthesized DA from the roots of Angelica gigas and performed HPLC and NMR analysis to confirm the structure and purity of DA (Supplementary Figure 1-A, B, C, D, E, F). Inflammation-inducer of phorbol ester origin such as TPA induces a similar type of chronic inflammatory symptoms and is also rooted in the development of different types of cancers (Tobias et al., 2016). After Topical application of TPA over a period of 4 days on mice ears, we observed a rush of inflammatory cell infiltration, comprising of the influx of polymorphonuclear leukocytes (neutrophils) on the site of inflammation which are primed by cytokines and mobilized by chemokines and the secretion of a various different pro-inflammatory cytokines and MHC class II molecules triggers the activation of T cells (Wright et al., 2010). The activated T-helper cells play a central role in the subsequent invasion of monocytes, which differentiate into tissue macrophages (Jinfang Zhu and Paul, 2008). The inflammatory reaction induced by TPA and different irritants can be quantified by measuring the ear weigh and ear thickness, appropriate for preliminary screening of anti-inflammatory drugs (He et al., 2013). We further investigated the molecular and cellular mechanisms of inflammation after TPA application on mice ears and performed histological, ELISA and western blotting analysis.

Our in-vivo experiment was able to substantiate the previously published papers of DA on an in-vitro anti-inflammatory model system. DA at both doses (10–25 mg/kg) was able to significantly inhibit TPA-induced ear inflammation, and subsequently suppress the activation of macrophages and infiltrating inflammatory cells. To further justify our experiment, we investigated the markers of macrophages and inflammatory cells such as ICAM-1, MIP-2, MCP-1, MIP-1β. The involvement of ROS and its role in various skin inflammatory diseases have been extensively studied (Bickers and Athar, 2006). So, we tested the potential role of DA to inhibit oxidative stress induced by application of TPA. The nitric oxide synthase enzymes, which catalyse the synthesis of nitric oxide, were significantly downregulated resulting in reduced free radical NO production upon DA treatment. MDA, which is one of the final products of polyunsaturated fatty acid peroxidation, overproduced by excessive free radicals in the cells was also significantly downregulated. DA administration was also able to enhance the activity antioxidant enzymes such as catalase, SOD-1, and SOD-2. The inactivation of NF-κB could be validated by the reduction of NF-κB p65 subunit and the down-regulation of NF-κB target genes such as TNF-α, IL-6 which was established through ELISA, staining and western blotting analysis, overall, leading to the repression of pro-inflammatory enzymes and cytokines. Conclusively, we suggest DA can be a good therapeutic compound for different kinds of inflammatory reactions on the skin and inflammation-related diseases. However, further more experiments would be required to validate the compound as a potent drug for clinical trials.

Conflicts of interest

The authors declare no competing financial interest.

Declaration of interests

There is no conflict of interest among the authors.

Acknowledgements

This research was financially supported by the Ministry SMEs and Startups(MSS), Korea, under the “Regional Specialized Industry Development Program (No. P0004934)” supervised by the Korea Institute for Advancement of Technology (KIAT) and “This work was supported by a grant from the Nakdonggang National Institute of Biological Resources (NNIBR), funded by the Ministry of Environment (MOE) of the Republic of Korea (NNIBR201902105)."

Transparency document

Transparency document related to this article can be found online at https://doi.org/10.1016/j.fct.2019.110699.

Appendix A. Supplementary data

Supplementary data to this article can be found online at https://doi.org/10.1016/j.fct.2019.110699.

References

Ahn, Eun Hee, Kim, Dae Won, Kang, Hye Won, Shin, Min Jae, Won, Moo Ho, Kim, Joon, Kim, Dong Joon, Kwon, Oh Shin, Kang, Tae Cheon, Han, Kyu Hyung, Park, Jinseu, Eum, Won Sik, Choi, Soo Young, 2010. Transduced PEP-1-ribosomal protein S3 (rpS3) ameliorates 12-O-tetradecanoylphorbol-13-acetate-induced inflammation in mice. Toxicology 276 192–197.

Barrera, G., 2012. Oxidative stress and lipid peroxidation products in cancer progression and therapy. Oncol 2012–137289.

Ben Neriah, Y., 2002. Regulatory functions of ubiquitination in the immune system. Nat. Immunol. 3, 20–26.

Bernatchez, Stephanie F., Atkinson, Matthew R., Parks, Patrick J., 1997. Expression molecule-l of intercellular adhesion on macrophages in vitro a marker of activation. Biomaterials 18, 1371–1378.

Bhatt, Dev, Ghosh, Sankar, 2014. Regulation of the NF-κB-Mediated transcription of inflammatory genes. Front. Immunol. 5, 71.

Bickers, D.R., Athar, M., 2006. Oxidative stress in the pathogenesis of skin disease. J. Investig. Dermatol. 126, 2565–2575.

Chauhan, A.K., Jakhar, R., Paul, S., Kang, S.C., 2014. Potentiation of macrophage activity by thymol through augmenting phagocytosis. Int. Immunopharmacol. 18 (2), 340–346.

Chen, J.T., Yang, C.R., 2004. Researches in Angelica L. Nat Prod Res Dev 16 (4), 359–365.

Chen, W., Zhang, W., Shen, W., Wang, K., 2010. Effects of the acid polysaccharide fraction isolated from a cultivated Cordycepssinensis on macrophages in vitro. Cell. Immunol. 262 (1), 69–74.

Degan, D., Ornello, R., Tiseo, C., Carolei, A., Sacco, S., Pistoia, F., 2018. The role of inflammation in neurological disorders. Curr. Pharmaceut. Des. 24 (14), 1485–1501.

Dey, D.K., Khan, I., Kang, S.C., 2019. Anti-bacterial susceptibility profiling of Weissella confusa DD_A7 against the multidrug-resistant ESBL-positive E. coli. Microb. Pathog. 128, 119–130.

Draper, H., Hadley, M., 1990. Malondialdehyde determination as index of lipid peroxidation. Methods Enzymol. 186, 421–431.

Firestein, G.S., 2003. Evolving concepts of rheumatoid arthritis. Nature 423, 356–361.

Grivennikov, Sergei I., Greten, Florian R., Karin, Michael, 2010. Immunity, inflammation, and cancer. Cell 140, 883–899.

Guadalupe, Sabio, Davis, Roger J., 2014. TNF and MAP kinase signaling pathways. Semin. Immunol. 26 (3), 237–245.

Ha, H.Y., Kim, Y., Ryoo, Z.Y., Kim, T.Y., 2006. Inhibition of the TPA induced cutaneous inflammation and hyperplasia by ECSOD. Biochem. Biophys. Res. Commun. 348, 450–458.

Hayden, M.S., Ghosh, S., 2012. NF-kB, the first quarter-century: remarkable progress and outstanding questions. Genes Dev. 26, 203–234.

He, X.Y., Liu, Q.C., Peng, W., Huang, Y.L., Wu, C.J., 2013. Bioactivities and serum pharmacochemistry of Qi-Wei-Xiao-Yan-Tang. Pharmaceutical Biology 51 (5), 629–634.

Islam, Salman Ul, Lee, Jung Ho, Adeeb, Shehzad, Ahn, Eun-Mi, Lee, You Mie, Lee, Young Sup, 2018. Decursinol angelate inhibits LPS-induced macrophage polarization through modulation of the NFκB and MAPK signaling pathways. Molecules 23, 1880.

Khan, A.Q., Khan, R., Qamar, W., Lateef, A., Rehman, M.U., Tahir, M., Ali, F., Hamiza, O.O., Hasan, S.K., Sultana, S., 2013. Geraniol attenuates 12-O-tetradecanoylphorbol-13-acetate (TPA)-induced oxidative stress and inflammation in mouse skin: possible role of p38 MAP Kinase and NF-κB. Exp. Mol. Pathol. 94 (3), 419–429.

Kim, Jung Hee, Jeong, Ji Hye, Jeon, Sung Tak, Ho, Kim, Jiyeon, Ock, Kyoungho, Suk, Kim, Sang In, Song, Kyung Sik, Lee, Won ha, 2006. Decursin inhibits induction of inflammatory mediators by blocking nuclear factor- κB activation in macrophages. Mol. Pharmacol. 69, 1783–1790.

Kim, Won Jung, Lee, Min Young, Kim, Jung Hee, Kyoungho, Suk, Lee, Won Ha, 2010. Decursinol angelate blocks transmigration and inflammatory activation of cancer cells through inhibition of PI3K, ERK and NF-κB activation. Cancer Lett. 296, 35–42.

Korhonen, R., Lathi, A., Kankaanranta, H., Moilanen, E., 2005. Nitric oxide production and signaling in inflammation. Curr. Drug Targets - Inflamm. Allergy 4, 471–479.

Lawrence, Toby, 2009. The nuclear factor NF-κB pathway in inflammation. Cold Spring Harb Perspect Biol 1 (6) a001651.

Lee, Sun Hwa, Kim, Dae Won, Eom, Seon Ae, Jun, Se Young, Park, Meeyoung, Kim, Duk Soo, Kwon, Hyung Joo, Kwon, Hyeok Yil, Han, Kyu Hyung, Park, Jinseu, Hwang, Hyun Sook, Won Sik Eum, Choi, Soo Young, 2012. Suppression of 12-O-tetradecanoylphorbol-13-acetate(TPA)-induced skin inflammation in mice by transduced Tat-Annexin protein. BMB Rep 45 (6), 354–359.

Li, Q., Verma, I.M., 2002. NF-κB regulation in the immune system. Nat. Rev. Immunol. 2, 725–734.

Li, X., Su, Y., Sun, J., Yang, Y., 2012. Chicken embryo extracts enhance spleen lymphocyte and peritoneal macrophages function. J. Ethnopharmacol. 144 (2), 255–260.

Libby, P., Ridker, P.M., Maseri, A., 2000. Inflammation and atherosclerosis. Circulation 105, 1135–1143.

Lim, Jongdoo, Kim, AIk Hwan, Kim, Hyeon Ho, Ahnc, Kyung Seop, Hogyu, Hana, 2001. Enantioselective syntheses of decursinol angelate and decursin. Tetrahedron Lett. 42, 4001–4003.

Liu, Ting, Zhang, Lingyun, Joo, Donghyun, Sun, Shao Cong, 2017. NF-κB signaling in inflammation. Signal Transduct Target Ther 2, 17023.

MacMicking, J., Xie, Q.W., Nathan, C., 1997. Nitric oxide and macrophage function. Annu. Rev. Immunol. 15, 323–350.

Mosser, D.M., Edwards, J.P., 2008. Exploring the full spectrum of macrophage activation. Nat. Rev. Immunol. 8, 958–969.

Nathan, C., Ding, A., 2010. Non resolving inflammation. Cell 140, 871–882.

Sengupta, A., Lichti, U.F., Carlson, B.A., Ryscavage, A.O., Gladyshev, V.N., 2010. Selenoproteins are essential for proper keratinocyte function and skin development. PLoS One 5 (8), e12249.

Shehzad, Adeeb, Islam, Salman Ul, Ahn, Eun Mi, Lee, You Mie, Lee, Young Sup, 2016. Decursinol angelate inhibits PGE2-induced survival of the human leukemia HL-60 cell line via regulation of the EP2 receptor and NF kB pathway. Cancer Biol. Ther. 17 (9), 985–993.

Shehzad, A., Parveen, S., Qureshi, M.,., Lee, Y.S., 2018. Decursin and decursinol angelate: molecular mechanism and therapeutic potential in inflammatory diseases. Inflammat. Res. 67, 209–218.

Song, H.Y., Lee, J.A., Ju, S.M., Yoo, K.Y., Won, M.H., Kwon, H.J., Eum, W.S., Jang, S.H., Choi, S.Y., Park, J., 2008. Topical transduction of superoxide dismutase mediated by HIV-1 Tat protein transduction domain ameliorates 12-O-tetradecanoylphorbol-13-acetate (TPA)-induced inflammation in mice. Biochem. Pharmacol. 75, 1348–1357.

Stanley, P.L., Steiner, S., Havens, M., Tramposch, K.M., 1991. Mouse skin inflammation induced by multiple topical applications of 12-O-tetradecanoylphorbol-13-acetate. Skin Pharmacol. 4, 262–271.

Straub, Rainer H., Schradin, Carsten, 2016. Chronic inflammatory systemic diseases: an evolutionary trade-off between acutely beneficial but chronically harmful programs. Evolut., Med. Publ. Health 37–51.

Sullivan, G.W., Sarembock, I.J., Linden, J., 2000. The role of inflammation in vascular diseases. J. Leukoc. Biol. 67 (5), 591–602.

Tang, Lihua, Wang, Kepeng, 2016. Chronic inflammation in skin malignancies. J. Mol. Signal. 11 (2), 1–13.

Tobias, Bald, Landsberg, Jennifer, Jansen, Philipp, Gaffal, Evelyn, Thomas, Tuting, 2016. Phorbol ester-induced neutrophilic inflammatory responses selectively promote metastatic spread of melanoma in a TLR4-dependent manner. OncoImmunology 5 (2) e1078964.

Wang, Cathy, Steer, James H., Joyce, David A., Yip, Kirk Hm, Zheng, Ming H., Xu, Jiake, 2003. 12-O-tetradecanoylphorbol-13-acetate (TPA) inhibits osteoclastogenesis by suppressing RANKL-induced NF-κB activation. J. Bone Miner. Res. 18 (12), 2159–2168.

Wright, H.L., Moots, R.J., Bucknall, R.C., Edwards, S.W., 2010. Neutrophil function in inflammation and inflammatory diseases. Rheumatology 49, 1618–1631.

Yang, E.J., Song, G.Y., Lee, J.S., Yun, C.Y., Kim, I.S., 2009. A novel (S)-(+)- decursin derivative, (S)-(+)-3-(3,4-dihydroxy-phenyl)-acrylic acid 2,2-dimethyl-8-oxo-3,4-dihydro-2H,8H-pyrano[3,2-g]chromen-3- yl-ester, inhibits ovalbumin-induced lung inflammation in a mousemodel of asthma. Biol. Pharm. Bull. 32, 444–449.

Zhang, Ping, Martin, Michael, Michalek, Suzanne M., Katz, Jannet, 2005. Role of mitogen-activated protein kinases and NF-κB in the regulation of proinflammatory and anti-inflammatory cytokines by porphyromonas gingivalis hemagglutinin B. Infect. Immun. 73 (7), 3990–3998.

Zhang, Qian, Lenardo, Michael J., Baltimore, David, 2017. 30 years of NF-κB: a blossoming of relevance to human pathobiology. Cell 168 (1–2), 37–57.

Zhu, Jinfang, Paul, William E., 2008. CD4 T cells: fates, functions, and faults. Blood 112, 1557–1569.